Front. Earth Sci. 2023, 17(3): 691−700
https://doi.org/10.1007/s11707-022-1019-9

RESEARCH ARTICLE

Pore structure evolution of mudstone caprock under cyclic load-unload and its influence on breakthrough pressure

Junchang SUN[1], Zhiqiang DONG[2], Sinan ZHU[3], Shifeng TIAN[2], Junping ZHOU (✉)[2]

1 Bohai Rim Energy Research Institute, Northeast Petroleum University, Qinghuangdao 066004, China
2 State Key Laboratory of Coal Mine Disaster Dynamics and Control, Chongqing University, Chongqing 400044, China
3 Sinopec Petroleum Exploration and Production Research Institute, Beijing 100083, China

Abstract The pore structure of caprock plays an important role in underground gas storage security, as it significantly influences the sealing capacity of caprock. However, the pore structure evolution of caprock with the cyclic stress perturbations triggered by the cyclic gas injection or extraction remains unclear. In this study, the pore structure changes of mudstone caprock under cyclic loading and unloading were obtained by the nuclear magnetic resonance (NMR) tests system, then the influence of the changes on the breakthrough pressure of caprock was discussed. The results indicated that the pore structure changes are depending on the stress loading-unloading path and stress level. In the first cyclic, at the loading stage, with the increase of confining stress, the NMR T_2 spectra curve moved to the left, the NMR signal amplitude of the first peak increased, while the amplitude of the second peak decreased gradually. This indicated that the larger pores of mudstone are compressed and transformed into smaller pores, then the number of macropores decreased and the number of micro- and meso-pores increased. For a certain loading-unloading cycle, the porosity curve of mudstone in the loading process is not coincide with that in the unloading process, the porosity curve in the loading process was located below that in the unloading process, which indicated that the pore structure change is stress path dependent. With the increase of cycle numbers, the total porosity shown an increasing trend, indicating that the damage of mudstone occurred under the cyclic stress load-unload effects. With the increase of porosity, the breakthrough pressure of mudstone decreased with the increase of the cyclic numbers, which may increase the gas leakage risk. The results can provide significant implication for the underground gas storage security evaluation.

Received January 18, 2022; accepted April 11, 2022

E-mail: zhoujp1982@sina.com

Keywords underground gas storage, pore structure, nuclear magnetic resonance, cyclic loading-unloading, breakthrough pressure

1 Introduction

Storage of gas (CH_4, CO_2, H_2) in subsurface formation has emerged as a promising means of large-scale, long-term, cost-effective energy storage, which allows for balancing energy supply and demand, increasing the energy security (Wang and Economides, 2012; Astiaso Garcia et al., 2016; Parra et al., 2019; Xu et al., 2022) . Potential subsurface formations include depleted natural gas or oil reservoirs, deep saline aquifers, and salt caverns (Paluszny et al., 2020; Cheng et al., 2021; Liu et al., 2021; Fan et al., 2022). Depleted gas or oil reservoirs are the most commonly used for underground natural gas storage, which is also capable of storing CO_2 and H_2. Adapting depleted gas and oil reservoirs for underground gas storage requires lower costs than in the aquifers or salt caverns, as it can decrease the early geological exploration cost and utilize the original facilities of oil and gas fields. What is more, the sealing capacity of the formation is confirmed by the existence of a natural gas reservoir (Matos et al., 2019; Tarkowski, 2019) .

The security of gas storage in depleted gas and oil reservoirs is strongly dependent on the sealing capacity of the caprock. Ideal candidate sites for the gas storage should be covered by poorly permeable caprock, which prevents gas leakage toward the surface (Shukla et al., 2010). During the gas storage, the cyclic injection-extraction of gas will induce the cyclic stress perturbations in formation, then impact the storage capacity and overall safety of the system (Carneiro et al., 2019; Zhang et al., 2019c). The cyclic stress perturbations will induce the caprock deformation, causing the pore structure alterations in caprock, then affecting the sealing

capacity and gas breakthrough pressure of the caprock (Ma et al., 2010; Kawaura et al., 2013; Fan et al., 2022). However, the dynamic pore structure evolution of caprock with the cyclic stress perturbations triggered by the cyclic gas injection-extraction remains undetermined, and its influence on the gas breakthrough pressure requires further studies (Pang et al., 2012; Tang et al., 2021).

At present, there are many methods to characterize the pore structure of rock material, such as mercury porosimetry (MIP) (Li et al., 2018a), gas adsorption (N_2/CO_2) (Jiang et al., 2019), scanning electron microscopy (SEM) (Zhang et al., 2022), small angle scattering techniques and μ-CT scanning (Wang et al., 2020). However, most of these methods remain unavailable for pore structure characterization at *in situ* stress conditions, especially for the cyclic stress loading-unloading conditions. The nuclear magnetic resonance (NMR) method has the advantages of being non-destructive, fast, and accurate, which is available for *in situ* pore structure characterization of rock. T_2 spectra measured by low-field NMR can effectively characterize the pore size distribution and porosity in rock material (Gao and Li, 2016; Schmitt et al., 2017; Li et al., 2018b; Zheng et al., 2020; Wang et al., 2021). Therefore, in this paper, the nuclear magnetic resonance (NMR) testing method is used to study the dynamic evolution of pore structure in mudstone caprock at the cyclic confining stress loading-unloading, then its influence on the breakthrough pressure of mudstone caprock was discussed. The results can provide significant implications in the gas storage security and risk evaluation.

2 Materials and methods

2.1 Sample preparation

The selected sample is a cylinder mudstone with a diameter of 25 mm and a height of 50 mm, which was obtained from a caprock of a natural gas reservoir with a buried depth of 3000 m, for the gas reservoir, the thickness of the caprock is about 150 m. The mineral compositions of the mudstone caprock obtained by X-ray diffraction analysis and its initial porosity and permeability are shown in Table 1. It can be seen that the mudstone is mainly composed of quartz, plagioclase, and clay minerals, among which the clay mineral content is the highest with a content of 53%. The initial porosity and permeability of mudstone are extremely low, which show favorable properties as a caprock.

2.2 Experimental section

The dynamic pore structure evolution of water-saturated mudstone caprock at different cyclic confining stress loading-unloading was obtained by the MacroMR12-150H-I NMR core micro-nondestructive testing imaging and analysis system (Suzhou Newmai Analytical Instruments Co., Ltd.), as shown in Fig. 1. The system is composed of several subsystems, including a ZYB-II vacuum pressure saturation device (a), an antimagnetic core holder (b), NMR monitoring system (c), a data acquisition system (d), and an HXH-100B double-cylinder constant-flow and constant-pressure pump to provide confining stress for cycle loading-unloading (e).

To simulate the cyclic gas injection-extraction induced stress perturbations in formation during the gas storage processes, the mudstone was subjected to cyclic stress loading-unloading, with 50 cycles in total. Considering the mechanical properties of the sample, the min and max confined stress of the mudstone sample in the loading-unloading process was set as 2 MPa and 18 MPa, respectively, with the single-cycle stress loading-unloading path of 2-10-18-10-2 MPa. The NMR test data (transverse relaxation time T_2 distribution) corresponding to the min confining stress (2 MPa), the intermediate confining stress (10 MPa), and the max confining stress (18 MPa) at the 1st, 10th, 20th, 30th, 40th, and 50th loading-unloading cycle were recorded. The test scheme is shown in Fig. 2.

The application of NMR in studying the pore structure of rock material is based on the fact that the ^{1}H relaxation time is positively correlated with pore size, thus, the tested sample is fully saturated with degassed pure water for at least 24 h in this study. The relationship between the T_2 and the pore size of rock can be expressed as (Yao et al., 2010):

$$\frac{1}{T_2}=\frac{1}{T_{2s}}=\rho\left(\frac{S}{V}\right)_{\text{pore}}=F_s\frac{\rho}{r}, \tag{1}$$

where T_2 is transverse relaxation time; T_{2s} represents the surface relaxation time; ρ is the transverse surface relaxation intensity. S is pore surface area, V is pore volume; F_s is the geometry factor (dimensionless), which is related to pore geometrical model, for spherical pores,

Table 1 Mineral compositions, and initial porosity and permeability parameters of mudstone sample

Core sample	The X-ray diffraction analysis					Initial porosity and permeability	
	Quartz/%	Plagioclase/%	Calcite/%	Clay minerals/%	Others/%	Porosity/%	Permeability/10^{-3} μm^2
Mudstone	33.2	16.2	0.9	37.2	12.5	0.78	0.00240

Note: clay minerals are the total amount of kaolinite, montmorillonite, illite, and chlorite.

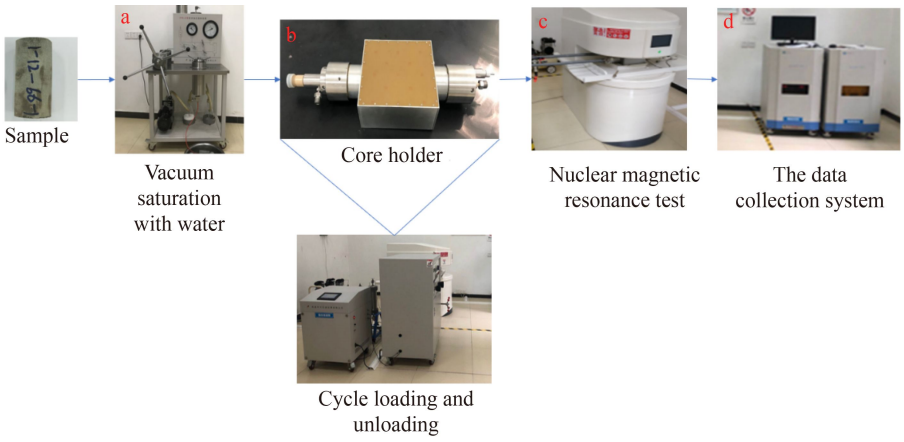

Fig. 1 The NMR measurement system.

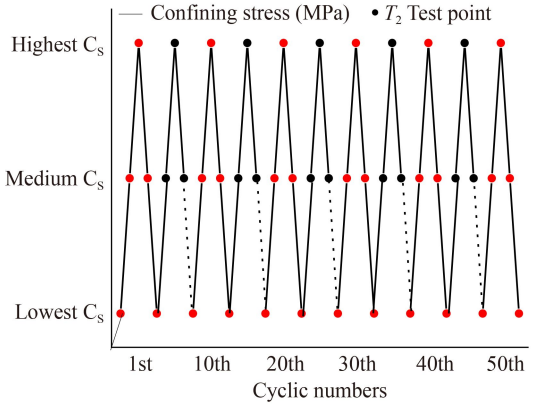

Fig. 2 Schematic of the experimental program (C_s = Confining stress).

F_s = 3, for cylindrical pores, F_s = 2; r is the pore radius. Based on the NMR test results, the pore size distribution during the cyclic loading-unloading processes can be obtained by the relationship between the pore size and T_2, the porosity of the measured mudstone caprock can be obtained by comparing the T_2 spectra of a standard sample with a known porosity (Xu et al., 2019).

3 Results and discussion

3.1 T_2 spectra of caprock under different confining stress

The T_2 spectra of the mudstone sample under the first confining stress loading-unloading cycle is shown in Fig. 3. The T_2 value is positively correlated with the pore size of the rock, and the NMR T_2 amplitude is positively correlated with the number of pores, then the T_2 spectra can reflect the pore size distribution and the amount of the pore in the rock (Zhai et al., 2016; Zhao et al., 2022).

Based on the classification of pore size by the International Union of Pure and Applied Chemistry (IUPAC) (Sing, 1985), the pore of rocks can be divided into micropores (diameter < 2 nm), mesopores (2 nm < diameter < 50 nm), and macropores (diameter > 50 nm). It can be seen from Fig. 3 that during the loading-unloading process, the peak value of the T_2 spectra in mudstone and the corresponding relaxation time shown different change degrees with the variation in confining stress, but the overall shape shown little change. There are two peaks in the T_2 spectra of mudstone (Fig. 3(b)). The T_2 relaxation time of the first peak is 0.01–1.24 ms, and the NMR signal amplitude is much larger than that of

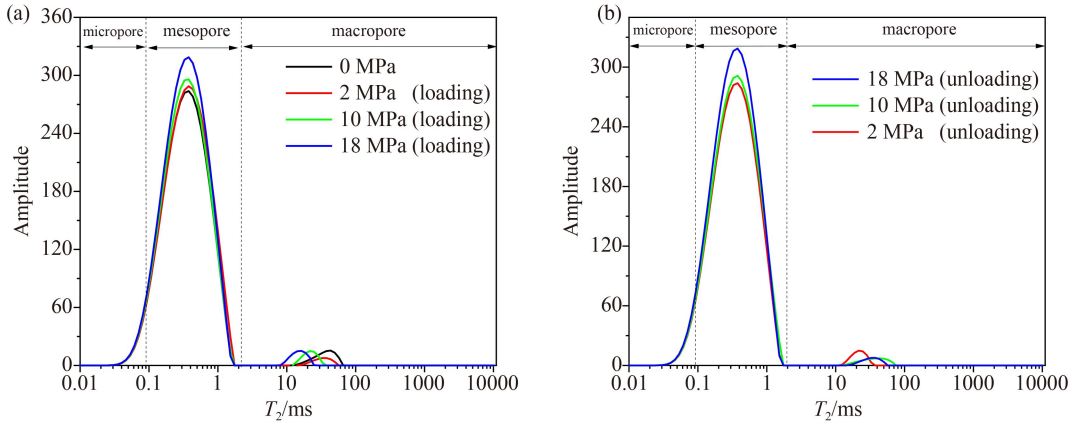

Fig. 3 T_2 spectra of mudstone under the first cyclic loading and unloading.

the second peak, indicating that the mudstone has more small pores and fewer large pores. However, the two peaks are discontinuous, reflecting that the pore connectivity in mudstone is poor (Li et al., 2016).

Under the impact of confining stress, the pore size distribution of mudstone shown changes with different degrees. In the loading stage, with the increase of confining stress, the T_2 spectra of mudstone shown a trend of moving to the left, the peak value of the first peak is increased, the peak value of the second peak and its corresponding T_2 values are gradually decreased, which indicated that the larger pores in the mudstone are compressed, and transformed into smaller (micro- and mesopores) under the compression of confining stress, resulting in an increase in the amount of smaller pores and a decrease in the amount of larger pores. In the unloading stage, the change of the first peak of mudstone with the confining stress is similar to that in the loading stage, while the second peak increased slightly and tends to shift to the right compared with the loading condition at the same stress level, indicating that although the deformation of mudstone have recovered to a certain extent after compression, it does not recover to the original state. Therefore, along the confining stress unloading path, the number of micropores corresponding to T_2 values in the range of 0.01–1.24 ms decreased with the unloading of confining stress, indicating that some micropores are transformed into larger pores due to the recovery of deformation, resulting in the decrease of the amount of micropores. Overall, during the loading and unloading processes, the change of the pore structure of mudstone is mainly caused by the compression of larger pores.

3.2 Influence of the cycle numbers on the pore structure of mudstone

3.2.1 T_2 spectra distribution of mudstone under different cyclic numbers

Under the cyclic loading-unloading, the T_2 spectra of mudstone sample at different confining stresses in the loading and unloading process are shown in Fig. 4. It can be seen from Fig. 4, for a certain cycle, at the same confining stress level, the T_2 spectra of mudstone sample in the loading and unloading processes is not coincide, indicating that the pore deformation is not completely restored in the unloading process. The T_2 value of the first peak at each confining stress level is 0.38 ms and its peak value are greater than that of the second peak, which indicates that there are more micropores in mudstone, and the cyclic loading-unloading path shows little impact on the micropores, while the T_2 value of the second peak is different at different confining stress condition. During the loading process, for the 1st, 10th, 20th and 30th cyclic loading, with the increase of confining stress, the amplitude of the first peak gradually increased, and the second peak shown a trend of moving to the left, indicating that the pore of mudstone is compressed, and the pore size become smaller so that the amount of micropores gradually increased. The second peak tends to move to the right (even the third peak appears under 10 MPa confining stress in the 50th cycle as shown in Fig. 4(f)), which may be due to some pores in the mudstone sample collapsed or some new micro-fissures generated under cyclic loading. The porosity of a rock is closely related to the internal microstructure and the minerals arrangement in it. At higher confining stress conditions, the flaky minerals and the unconformable contact structure are deformed, extruded and destroyed, then formed some new micro-fissures, or induced the non-connected pores and fissures transformed into connected (Li et al., 2018b; Wang et al., 2018; Zhang et al., 2019a).

In addition, the T_2 spectra of mudstone at the same confining stress level are not coincident for a certain loading-unloading cycle, indicating that the deformation of mudstone during the loading-unloading process is irreversible. The T_2 spectra of mudstone in the unloading stage is generally located on the right side of that in the loading stage, indicating that the mudstone is irreversibly damaged during the loading process at higher confining stress condition (Takeda and Manaka, 2018). Therefore, for a certain cycle at the same stress level, the pore diameters corresponding to different T_2 peak values in the unloading stage are generally higher than those in the loading stage.

It should be noted that the max confining stress of the cyclic loading-unloading process is not only the end of loading but also the start of unloading, the change of the T_2 spectra of mudstone under the max confining stress level (18 MPa) with the increase of cycle numbers is shown in Fig. 5. At the first loading process, the macro-pores in the mudstone are compressed, with the increase of the cycle numbers, the peak values of the two peaks in mudstone increased after multiple cyclic loading-unloading, indicating that the mudstone is damaged by multiple cyclic loading-unloading, resulting in the generation of new pores and fissures. In the process of cyclic loading-unloading, the deformation of mudstone is mainly composed of recoverable elastic deformation and non-recoverable plastic deformation. Thus, the deformation of mudstone in the cyclic loading-unloading processes is closely related to the stress path and stress level.

3.2.2 Variation of pore structure parameters with cycle numbers

The pore structure parameters of mudstone at different cycle numbers are shown in Table 3 and Fig. 6.

As shown in Fig. 6(d), with the increase of cycle

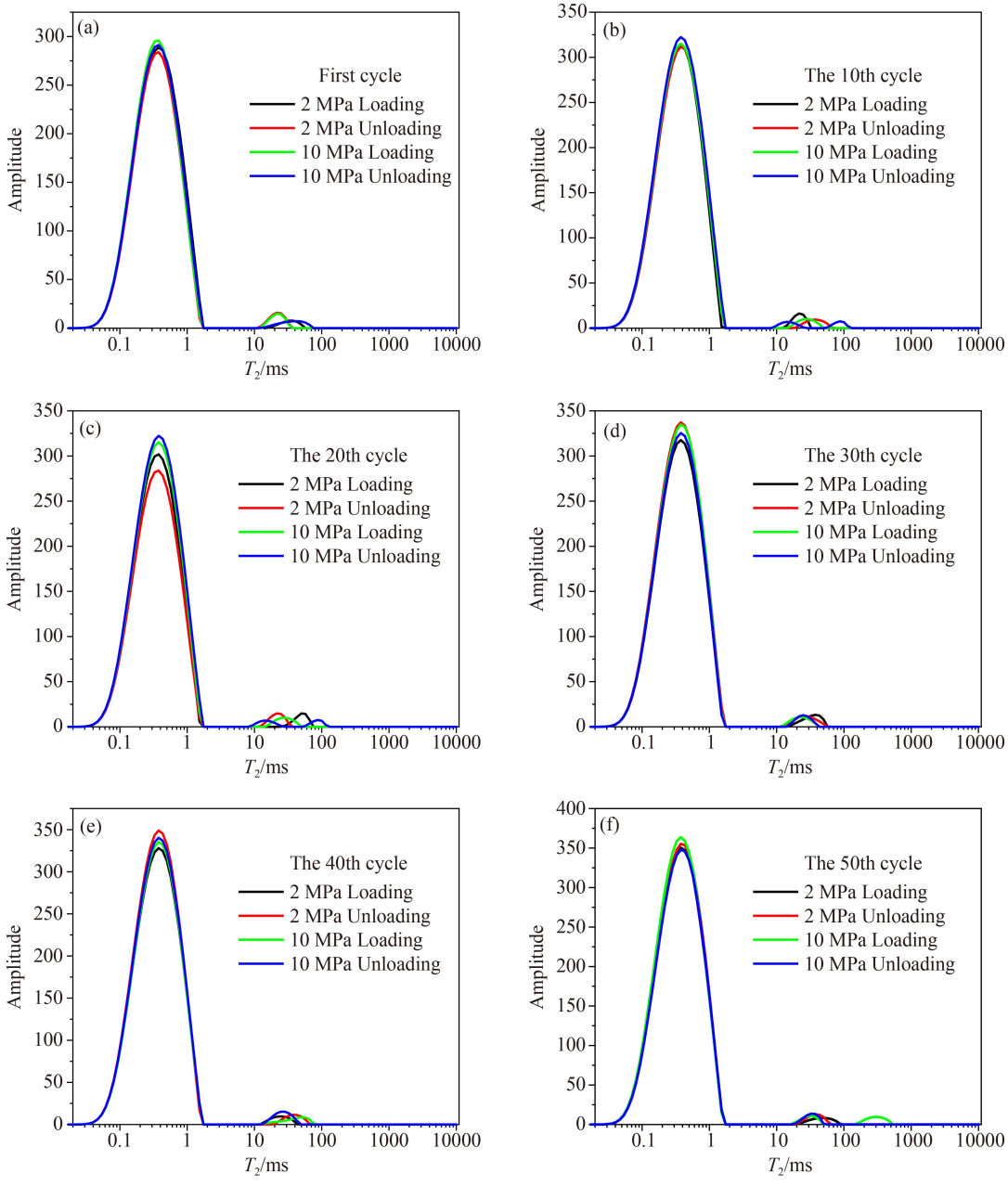

Fig. 4 T_2 spectra of mudstone under different cycle numbers of loading and unloading.

numbers, in the process of the loading process, the porosity of mudstone decreased first and then increased with the increase of confining stress, while in the unloading process, the porosity of mudstone increased first and then decreased with the decrease of confining stress. Under the confining stress condition of 18 MPa, the proportion of larger pores in mudstone is relatively high, indicating that irreversible plastic deformation and damage occur in mudstone under the condition of higher confining stress (Xu et al., 2006; Chao et al., 2017), and new pore and fracture structures are generated, then increased the porosity. With the increase of cycle numbers, the micropore, mesopore, and total pore volume of mudstone show an increasing trend. Under the same confining stress level, the proportion of macropore decreased gradually, while the proportion of micropore and mesopore increased. In addition, for any certain loading-unloading process, the porosity of mudstone at the same confining stress level does not coincide, which shows a similar hysteresis phenomenon with the hysteresis behavior of the stress-strain curve during the cyclic loading-unloading process. For any certain cycle, the porosity of mudstone in the loading process is lower than that of in the unloading process, which is also related to the change of mudstone porosity in any single loading process, indicating that the stress loading path shows significant impact on the pore structure change of mudstone (Zhang et al., 2019b; Liu et al., 2021). Under

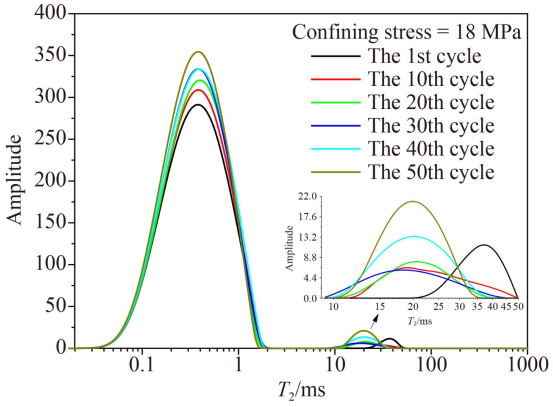

Fig. 5 T_2 spectra of mudstone under max confining stress with different cyclic numbers.

the higher confining stress (18 MPa) condition, the damage is occurred in mudstone, when the confining stress is unloaded to 10 MPa, the porosity of mudstone is larger than that of the previous loading process at the stress of 10 MPa. While in the unloading process, the porosity at the confining stress of 2 MPa is less than that at the 10 MPa, which can be attributed to the redistribution of water in the pore structure of mudstone during the nuclear magnetic resonance test. In the unloading process, with the recovery of elastic deformation of mudstone, the water in larger pores will diffuse to smaller pores and reduce the water saturation of larger pores, which may result in a decrease in the corresponding measured porosity in mudstone (Chu et al., 2021).

The dynamic change of pore structure of caprock under cyclic loading-unloading will significantly affect the sealing capacity of caprock (Lv et al., 2017; Jayasekara et al., 2020). As shown in Figs. 6(a)–6(c), the accumulative amplitudes of different kinds of pores have an upward trend with the increase of cyclic numbers, and the total pore volume also increase, it is obvious that the value of accumulative amplitudes under the min and middle confining stress are lower than that under the max confining stress. The pore size distribution and porosity of caprock are important factors affecting its sealing capacity and breakthrough pressure. Generally, the larger the porosity of caprock is, the lower the breakthrough pressure is, and the breakthrough pressure decreases with the increase of the proportion of macropores and increases with the increase of the proportion of micropores and mesopores (Hu et al., 2021). The above experimental results in this study showed that the proportions of micropores, mesopores, and macropores in the caprock changed correspondingly during the cyclic loading-unloading processes. After a certain number of cycles, under a certain confining stress, the proportions of micropores and mesopores in the mudstone caprock increased, while the proportion of macropores decreased, then increase the breakthrough pressure of mudstone. However, it should be noted that under the higher confining stress condition, mudstone may be damaged and new pores and fractures can be generated, then the increase in the proportion of larger pores and total porosity is expected, causing the reduction in breakthrough pressure. In addition, as the pore structure changes are depending on the stress loading-unloading path and stress level, then the breakthrough pressure of rock is also stressed path-dependent (Lei et al., 2019). Thus, the influence of cyclic loading-unloading on the breakthrough pressure is controlled by multiple factors.

3.3 Influence of pore structure changes on the breakthrough pressure of mudstone caprock

Generally, the gas breakthrough in caprock is a complex process involving multiple phases and can be affected by many factors, such as the pore structure and porosity

Table 2 Variation of pore structure parameters of mudstone under cyclic loading-unloading

Confining stress		1st		10th		20th		30th		40th		50th	
		load	unload	load	unload	load	unload	load	unload	load	unload	load	unload
2 MPa	Micropore/%	4.64	4.38	4.29	4.30	4.56	4.60	4.40	4.37	4.38	4.34	4.31	4.20
	Mesopore/%	94.03	93.27	93.92	94.40	94.00	93.65	93.87	93.99	94.35	94.30	94.47	94.43
	Macropore/%	1.33	2.35	1.79	1.30	1.44	1.74	1.73	1.64	1.27	1.36	1.22	1.36
	Porosity/%	0.45	0.44	0.55	0.48	0.55	0.59	0.59	0.69	0.6	0.64	0.68	0.71
10 MPa	Micropore/%	4.47	4.58	4.39	4.36	4.37	4.36	4.30	4.37	6.46	4.28	4.42	4.23
	Mesopore/%	93.66	93.98	94.05	94.27	94.03	94.38	94.23	94.23	94.03	92.20	93.86	94.33
	Macropore/%	1.86	1.44	1.56	1.37	1.60	1.26	1.47	1.60	1.35	1.87	1.25	1.30
	Porosity/%	0.43	0.45	0.51	0.59	0.54	0.61	0.58	0.62	0.62	0.74	0.65	0.79
18 MPa	Micropore/%	4.45	4.27	4.22	4.30	4.23	4.38	4.45	4.27	4.22	4.30	4.23	4.38
	Mesopore/%	94.62	94.77	94.92	94.85	94.24	93.60	94.62	94.77	94.92	94.85	94.24	93.60
	Macropore/%	0.93	0.96	0.87	0.85	1.53	2.02	0.93	0.96	0.87	0.85	1.53	2.02
	Porosity/%	0.47	0.47	0.54	0.54	0.55	0.55	0.56	0.56	0.63	0.63	0.66	0.66

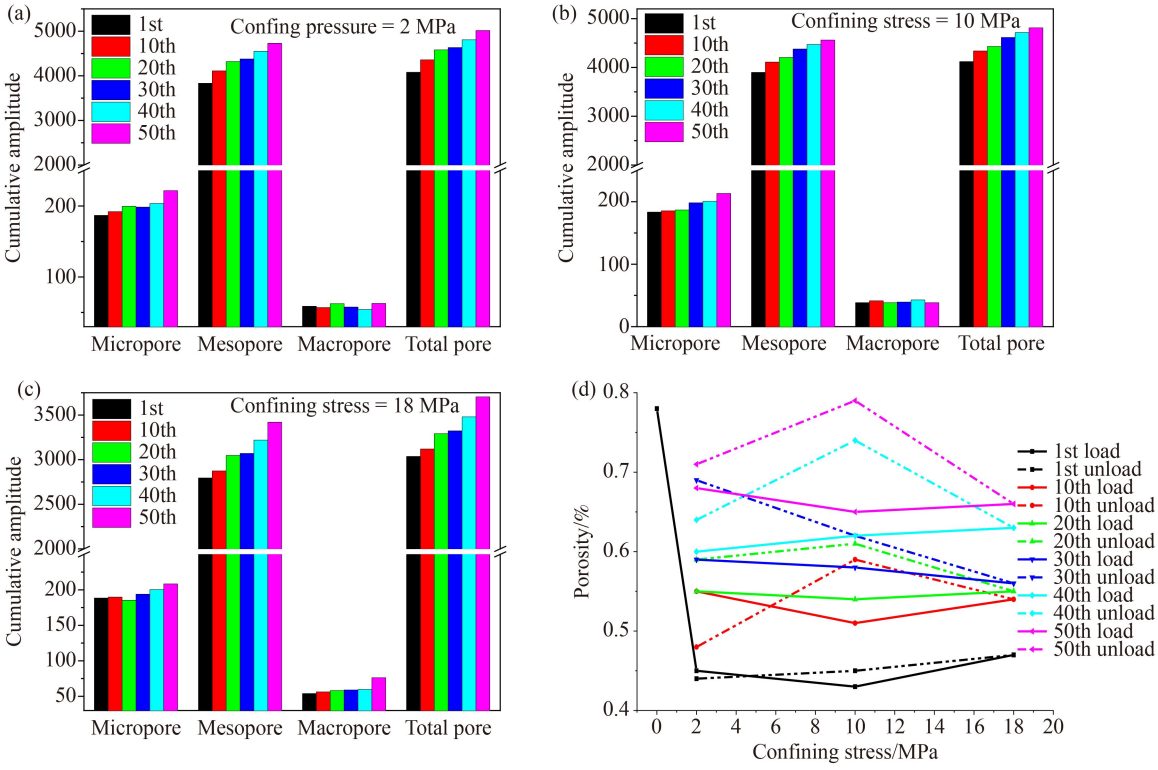

Fig. 6 Variation of pore structure parameters in mudstone at multiple cyclic loading-unloading.

(Zhang and Wang, 2022). Based on the existing studies, there is a relationship between breakthrough pressure and porosity and permeability, which can be expressed as (Wu et al., 2020)

$$P_t = \frac{\sigma}{\sqrt{\xi F}}\sqrt{\frac{1}{\phi k}}, \tag{2}$$

where P_t is breakthrough pressure, MPa, σ is surface tension, ξ is shape factor, F is formation resistivity coefficient, ϕ is porosity, and k is permeability, mD.

The relation between permeability k and porosity ϕ can be expressed as follows (Cui and Bustin, 2005):

$$k = k_0\left(\frac{\phi}{\phi_0}\right)^3, \tag{3}$$

where k_0 is the rock's initial permeability and ϕ_0 is the rock's initial porosity. Defining the relative breakthrough pressure as P_t/P_0, and ignoring the changes of rock surface tension, shape factor, and formation resistivity in the cyclic loading-unloading process, based on the pore structure and porosity changes in the cyclic loading-unloading process, the change of relative breakthrough pressure P_t/P_0 in the cyclic loading-unloading process can be expressed as follows:

$$\frac{P_t}{P_0} = \sqrt{\frac{\phi_0 k_0}{\phi_t k_t}}. \tag{4}$$

Substitute Eq. (3) into Eq. (4), the following equation can be obtained:

$$\frac{P_t}{P_0} = \frac{\phi_0^2}{\phi_t^2}. \tag{5}$$

Thus, according to the porosity change of mudstone induced by cyclic loading-unloading in this study, the breakthrough pressure changes with the cyclic loading-unloading can be obtained by using Eq. (5). Figure 7 shows the relationship between the relative breakthrough pressure, porosity, and permeability of mudstone caprock. It can be seen from Fig. 7 that the relative breakthrough pressure increased gradually with the decrease of porosity and permeability induced by cyclic loading-unloading, which is consistent with the results of (Zhou et al., 2019).

Figure 8 depicts the relationship between relative breakthrough pressure and between confining stress and the cycle numbers. As shown in Fig. 8, with the increase of confining stress, the pore volume of mudstone decreased, and the relative breakthrough pressure increased gradually. With the increase of the cycle numbers, as the cyclic loading-unloading causes micro-damage in the mudstone caprock, the mesopores, micropores, and total porosity show an increasing trend, then the relative breakthrough pressure decreased gradually. Therefore, it can be concluded that the breakthrough pressure of mudstone caprock decrease with the increase of the cycle numbers.

It should be noted that for a certain geological

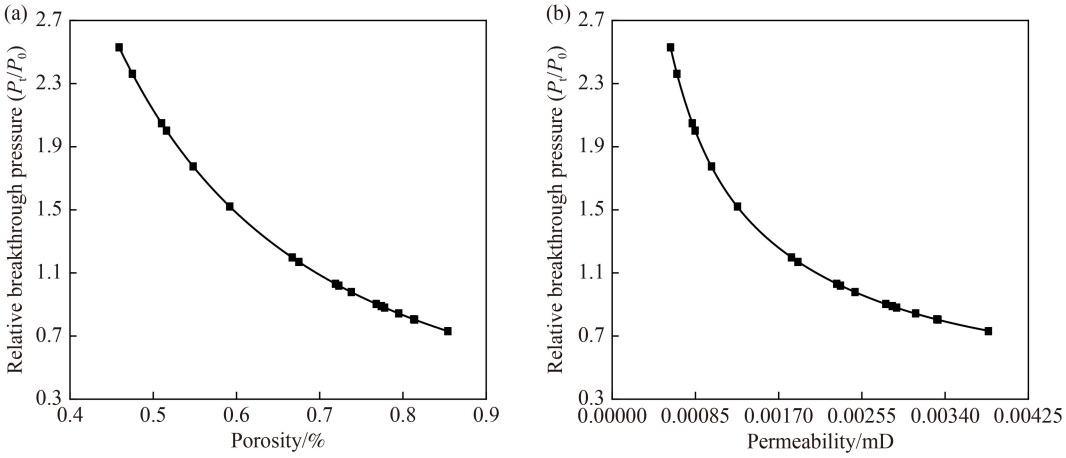

Fig. 7 The relationship between relative breakthrough pressure and porosity (a) and permeability (b) of mudstone caprock.

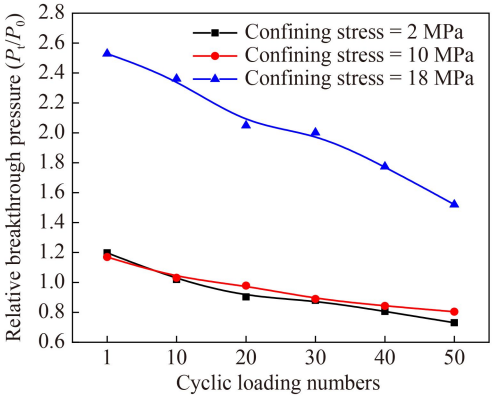

Fig. 8 Relationship between relative breakthrough pressure and confining stress and the cyclic loading numbers.

formation, when using to storage different gas (CH_4, CO_2, H_2), the alteration in breakthrough pressure of them with the cyclic stress maybe different, as they show different interfacial tension and wettability behaviors in the gas-water-rock system. The Washburn equation implies that the capillary entry pressure for a certain gas is positively related to interfacial tension and contact angle value (Hildenbrand et al., 2004). The interfacial tension for the H_2-water system may be similar that for the CH_4-water system as both gases have low aqueous solubilities in water. However, breakthrough pressure of CO_2 can be significantly influenced by the CO_2-brine-rock interactions. CO_2 can be dissolved in brine to form acid solution, then, the pore structure and minerals of the rock can be altered by the CO_2-brine-rock interactions, inducing the alteration in wettability behaviors of rock, which further affect the breakthrough pressure of CO_2 in it.

4 Conclusions

Based on the *in situ* nuclear magnetic resonance (NMR) test technology, the pore structure evolution of mudstone caprock under cyclic loading-unloading is obtained, and its influence on the gas breakthrough pressure was discussed, the main conclusions are as follows.

1) During the loading process, with the increase of confining stress, the T_2 spectra of mudstone caprock shown a trend of move to the left, the first peak amplitude increased, while the second peak amplitude and its corresponding T_2 value decreased, indicating that the macropores are compressed and transformed into micro and mesopores, resulting in the decrease in the volume of macropores and the increase in the amount of micro- and mesopores. In the loading-unloading process, the pore structure changes in the mudstone are mainly caused by the compression of larger pores.

2) In the loading process, the porosity decreased first and then increased, which indicates that the mudstone is damaged at a higher confining stress level. Under the same confining stress, the porosity curves in the loading and unloading process do not coincide, indicating that the mudstone has experienced irreversible deformation, the porosity in any loading process is less than that in the unloading process. With the increase of cycle numbers, the pore volume of micropore, mesopore, and the total porosity in mudstone shown an increasing trend, indicating the damage of rock is enhanced under multiple cyclic loading-unloading.

3) The breakthrough pressure of caprock is closely related to its pore size distribution, as the porosity and pore structure alteration of caprock is depending on the cyclic stress load-unload path and cycle numbers, thus the breakthrough pressure is also stress-dependent. The breakthrough pressure of mudstone decreased with the increase of the cycle numbers. In addition, the breakthrough pressure is also related to the gas type, the breakthrough pressure considering pore structure and gas-rock interaction should be further studied.

Acknowledgments This study was financially supported by the National Natural Science Foundation of China (Grant No. 52174107), the Basic Research and Frontier Exploration Projects in Chongqing (No. cstc2021 yszx-jcyjX0010).

References

Astiaso Garcia D, Barbanera F, Cumo F, Di Matteo U, Nastasi B (2016). Expert opinion analysis on renewable hydrogen storage systems potential in Europe. Energies, 9(11): 963

Carneiro J F, Matos C R, van Gessel S (2019). Opportunities for large scale energy storage in geological formations in mainland Portugal. Renew Sustain Energy Rev, 99: 201–211

Chao Z, Wang H, Xu W, Ji H, Zhao K (2017). Study on the evolution of permeability and porosity of columnar joint materials under cyclic loading and unloading. Chinese J Rock Mech Eng, 36(1): 124–141 (in Chinese)

Cheng L, Li D, Wang W, Liu J (2021). Heterogeneous transport of free ch_4 and free CO_2 in dual-porosity media controlled by anisotropic *in situ* stress during shale gas production by CO_2 flooding: implications for CO_2 geological storage and utilization. ACS Omega, 6(40): 26756–26765

Chu Z, Wu Z, Liu Q, Weng L, Wang Z, Zhou Y (2021). Evaluating the microstructure evolution behaviors of saturated sandstone using NMR testing under uniaxial short-term and creep compression. Rock Mech Rock Eng, 54(9): 4905–4927

Cui X, Bustin R M (2005). Volumetric strain associated with methane desorption and its impact on coalbed gas production from deep coal seams. AAPG Bull, 89(9): 1181–1202

Fan C, Wen H, Li S, Bai G, Zhou L (2022). Coal seam gas extraction by integrated drillings and punchings from the floor roadway considering hydraulic-mechanical coupling effect. Geofluids, 2022: 1–10

Gao H, Li H A (2016). Pore structure characterization, permeability evaluation and enhanced gas recovery techniques of tight gas sandstones. J Nat Gas Sci Eng, 28: 536–547

Hildenbrand A, Schlömer S, Krooss B M, Littke R (2004). Gas breakthrough experiments on pelitic rocks: comparative study with N_2, CO_2 and CH_4. Geofluids, 4(1): 61–80

Hu J, Dong Z, Ma S, Qin X, Xiao X, Zhuan D (2021). Seepage characteristics of damaged rock under stress-seepage coupling. Gold Sci Tech, 29(3): 355–363

Jayasekara D W, Ranjith P G, Wanniarachchi W, Rathnaweera T D (2020). Understanding the chemico-mineralogical changes of caprock sealing in deep saline CO_2 sequestration environments: a review study. J Supercrit Fluid, 161: 104819

Jiang J, Yang W, Cheng Y, Zhao K, Zheng S (2019). Pore structure characterization of coal particles via MIP, N_2 and CO_2 adsorption: effect of coalification on nanopores evolution. Powder Technol, 354: 136–148

Kawaura K, Akaku K, Nakano M, Ito D, Takahashi T, Kiriakehata S (2013). Examination of methods to measure capillary threshold pressures of pelitic rock samples. Energy Procedia, 37: 5411–5418

Lv X, Wang Y, Yu H, Bai Z (2017). Major factors affecting the closure of marine carbonate caprock and their quantitative evaluation: a case study of Ordovician rocks on the northern slope of the Tazhong uplift in the Tarim Basin, western China. Ma Pet Geol, 83: 231–245

Lei R, Wang Y, Zhang L, Liu B, Long K, Luo P, Wang Y K (2019). The evolution of sandstone microstructure and mechanical properties with thermal damage. Energy Sci Eng, 7(6): 3058–3075

Li H, Yang D, Zhong Z, Sheng Y, Liu X (2018b). Experimental investigation on the micro damage evolution of chemical corroded limestone subjected to cyclic loads. Int J Fatigue, 113: 23–32

Li J, Zhou K, Liu W, Deng H (2016). NMR research on deterioration characteristics of microscopic structure of sandstones in freeze–thaw cycles. Trans Nonferrous Met Soc China, 26(11): 2997–3003

Li X, Kang Y, Haghighi M (2018a). Investigation of pore size distributions of coals with different structures by nuclear magnetic resonance (NMR) and mercury intrusion porosimetry (MIP). Measurement, 116: 122–128

Liu J, Xie L Z, He B, Gan Q, Zhao P (2021). Influence of anisotropic and heterogeneous permeability coupled with *in-situ* stress on CO_2 sequestration with simultaneous enhanced gas recovery in shale: quantitative modeling and case study. Int J Greenh Gas Control, 104: 103208

Ma X, Yu B, Ma D, Zhang S, Cheng Y, Wang K, Yang Y (2010). Project design and matching technologies for underground gas storage based on a depleted sandstone gas reservoir. Nat Gas Ind, 30(8): 67–71

Matos C R, Carneiro J F, Silva P P (2019). Overview of large-scale underground energy storage technologies for integration of renewable energies and criteria for reservoir identification. J Energy Storage, 21: 241–258

Paluszny A, Graham C C, Daniels K A, Tsaparli V, Xenias D, Salimzadeh S, Whitmarsh L, Harrington J F, Zimmerman R W (2020). Caprock integrity and public perception studies of carbon storage in depleted hydrocarbon reservoirs. Int J Greenh Gas Control, 98: 103057

Pang J, Qian G, Wang B, Yang Z, Wei Y, Li Y (2012). Evaluation of sealing ability of underground gas storage converted from the Xinjiang H Gas Field. Nat Gas Ind, 32(2): 83–85

Parra D, Valverde L, Pino F J, Patel M K (2019). A review on the role, cost, and value of hydrogen energy systems for deep decarbonization. Renew Sustain Energy Rev, 101: 279–294

Schmitt M, Poffo C M, De Lima J C, Fernandes C P, Dos Santos V S S (2017). Application of photoacoustic spectroscopy to characterize thermal diffusivity and porosity of caprocks. Eng Geol, 220: 183–195

Shukla R, Ranjith P, Haque A, Choi X (2010). A review of studies on CO_2 sequestration and caprock integrity. Fuel, 89(10): 2651–2664

Sing K S W (1985). Reporting physisorption data for gas/solid systems with special reference to the determination of surface area and porosity. Pure Appl Chem, 57(4): 603–619

Takeda M, Manaka M (2018). Effects of confining stress on the semipermeability of siliceous mudstones: implications for identifying geologic membrane behaviors of argillaceous formations. Geophys Res Lett, 45(11): 5427–5435

Tang Y, Long K, Wang J, Xu H, Wang Y, He Y, Shi L, Zhu H (2021). Change of phase state during multi-cycle injection and production process of condensate gas reservoir based underground gas storage. Pet Explor Dev, 48(2): 395–406

Tarkowski R (2019). Underground hydrogen storage: characteristics and prospects. Renew Sustain Energy Rev, 105: 86–94

Wang G, Han D, Qin X, Liu Z, Liu J (2020). A comprehensive method for studying pore structure and seepage characteristics of coal mass based on 3D CT reconstruction and NMR. Fuel, 281: 118735

Wang L, Zhao N, Sima L, Meng F, Guo Y (2018). Pore structure characterization of the tight reservoir: systematic integration of mercury injection and nuclear magnetic resonance. Energy Fuels, 32(7): 7471–7484

Wang X L, Economides M J (2012). Purposefully built underground natural gas storage. J Nat Gas Sci Eng, 9: 130–137

Wang Z, Cui H, Wei G, Jia T, Guo J, He X (2021). Study on the quantitative characterization and seepage evolution characteristics of pores of loaded coal based on NMR. ACS Omega, 6(43): 28983–28991

Wu T, Pan Z, Connell L D, Liu B, Fu X, Xue Z (2020). Gas breakthrough pressure of tight rocks: a review of experimental methods and data. J Nat Gas Sci Eng, 81: 103408

Xu J, Xian X, Wang H, Wang w, Yang X (2006). Experimental study on rock deformation characteristics under cycling loading and unloading conditions. Chinese J Rock Mech Eng, 25(1): 3040–3045 (in Chinese)

Xu L, Li Q, Myers M, Chen Q, Li X (2019). Application of nuclear magnetic resonance technology to carbon capture, utilization and storage: a review. J Rock Mech Geotech Eng, 11(4): 892–908

Xu T, Tian H, Zhu H, Cai J (2022). China actively promotes: CO_2 capture, utilization and storage research to achieve carbon peak and carbon neutrality. Adv Geo-Energy Res, 6(1): 1–3

Yao Y, Liu D, Che Y, Tang D, Tang S, Huang W (2010). Petrophysical characterization of coals by low-field nuclear magnetic resonance (NMR). Fuel, 89(7): 1371–1380

Zhai C, Qin L, Liu S, Xu J, Tang Z, Wu S (2016). Pore structure in coal: pore evolution after cryogenic freezing with cyclic liquid nitrogen injection and its implication on coalbed methane extraction. Energy Fuels, 30(7): 6009–6020

Zhang C, Wang M (2022). A critical review of breakthrough pressure for tight rocks and relevant factors. J Nat Gas Sci Eng, 100: 104456

Zhang F, Jiang Z, Sun W, Li Y, Zhang X, Zhu L, Wen M (2019a). A multiscale comprehensive study on pore structure of tight sandstone reservoir realized by nuclear magnetic resonance, high pressure mercury injection and constant-rate mercury injection penetration test. Mar Pet Geol, 109: 208–222

Zhang L, Wang Y, Miao X, Gan M, Li X (2019c). Geochemistry in geologic-CO_2 utilization and storage: a brief review. Adv Geo-Energy Res, 3(3): 304–313

Zhang W, Ning Z, Gai S, Zhu J, Fan F, Liu Z, Wang H (2022). Fast and effective observations of the pore structure of tight sandstones at the same location by utilizing AFM and CF-SEM. J Petrol Sci Eng, 208: 109554

Zhang Z, Yu X, Deng M (2019b). Damage evolution of sandy mudstone mechanical properties under mining unloading conditions in gob-side entry retaining. Geotech Geol Eng, 37(4): 3535–3545

Zhao P, He B, Zhang B, Liu J (2022). Porosity of gas shale: is the NMR-based measurement reliable? Petrol Sci, 19(2): 509–517

Zheng S, Yao Y, Elsworth D, Wang B, Liu Y (2020). A novel pore size classification method of coals: investigation based on NMR relaxation. J Nat Gas Sci Eng, 81: 103466

Zhou X, Lu X, Quan H, Qian W, Mu X, Chen K, Wang Z, Bai Z (2019). Influence factors and an evaluation method about breakthrough pressure of carbonate rocks: an experimental study on the Ordovician of carbonate rock from the Kalpin area, Tarim Basin, China. Mar Pet Geol, 104: 313–330